PROCEEDINGS OF SPIE

SPIEDigitalLibrary.org/conference-proceedings-of-spie

Comparing a hyperspectral Monte-Carlo approach for simulating water surface reflectance signatures based upon radiative transfer theory: simulating clear water and Caribbean Sea bottom types

Charles R. Bostater, Manuel Gimond, Matthew Campbell

SPIE.

Comparing a hyperspectral Monte-Carlo approach for simulating water surface reflectance signatures based upon radiative transfer theory: simulating clear water & Caribbean Sea bottom types

Charles R. Bostater Jr.*, Manuel Gimond, Matthew Campbell
Marine Environmental Optics Laboratory & Remote Sensing Center
College of Engineering, Florida Tech

ABSTRACT

A homogeneous water column hyperspectral Monte Carlo modeling approach is compared to an analytical solution to a radiative transfer model system for irradiance. Both mathematical models and the solution approaches describe the transfer of irradiant light in a homogeneous medium. The analytical model has been previously used to describe the transfer of irradiant energy in a homogenous water column, with and without fluorescence source terms as well as a direct specular or a collimated irradiance source term. The response of the water surface reflectance under solar irradiance or an artificial collimated light source is thus modeled. Synthetic reflectance signatures generated from the 2 mathematical models describe the interaction of irradiant photon flux in terms of the 2 flow irradiance equations. The Monte Carlo model is used for creating synthetic coastal water color or reflectance signatures for clear waters with different bottom reflectance signatures using data collected in the Caribbean Sea region. The analytical model has suggested proportionality between the absorption and backscatter coefficients around 0.29. In this paper the proportionality factor for clear water using the Monte Carlo model of irradiance was found to vary, but averaged around 0.26. This compares to 0.33 from other published values used in simple remote sensing algorithms. Results suggest that the optical pathlength (the maximum distance a photon travels before interaction (scattering or absorption) within the medium) will be a dominant factor influencing the ability of the Monte Carlo model to accurately represent measured or known reflectance signatures. The hyperspectral Monte Carlo mathematical modeling results also suggest the value of the technique for calculating the backscattering coefficient in waters with varying suspended matter, dissolved organic matter (DOM) and phytoplankton pigments.

Keywords: reflectance spectroscopy, remote sensing, radiative transfer modeling, absorption coefficients, backscatter coefficients, environmental models, environmental surveillance, hyperspectral remote sensing, environmental optics, water surface reflectance, Monte Carlo techniques, 2 flow equations, remote sensing algorithms, hyperspectral optical signatures.

1. BACKGROUND

The two flow irradiance equations shown below, and the mathematical solution technique (with unique Cauchy type boundary conditions due to Bostater, Lamb & Ma[1,2] is used to compare a mathematically based Monte Carlo technique to generate synthetic hyperspectral water surface reflectance signatures. Both mathematical modeling approaches incorporate the influence of wavelength dependent specific backscatter & specific absorption coefficients and a wavelength dependent bottom reflectance signature. The terms in the hyperspectral Monte Carlo model approach are also wavelength dependent and also depend upon the constituents in the water column, such as suspended particulate matter, dissolved organic matter (DOM) and chlorophyll pigments. Simulations are used for predicting the response of the water surface reflectance under the influence of water constituents, as well the influences due to bottom types such as submerged corals, sand bottom types and sea grasses. Using previously published data by Smith and Baker[3], Bostater & Gimond[4] and Bostater[5], initial values of the wavelength specific absorption and backscatter terms are calculated and utilized along with downwelling irradiance from the atmosphere using atmospheric corrections similar to Ma[6] and Greg & Carder[7] as shown in Figure 1. The normalized cumulative

* Correspondence: Dr. Charles Bostater, 150 West University Blvd. Melbourne, Florida, USA, 32901
email: bostater@probe.ocn.fit.edu, http://www.ocn.fit.edu Telephone:321-258-9134 (Fax) 321-773-0980

downwelling irradiance curve shown in Figure 2 is used along with a random number generator due to Bostater[8] and Wichmann and Hill[9]. The interaction of a photon with the medium can take the form of an absorption event or backscattering event after entering the water column. Whether the photon interacts in terms of absorption, backscatter or forward scattering depends upon a random number generation procedure. The optical pathlength described below determines the approximate maximum distance a photon travels before an interaction event occurs. If the photon travels to the bottom depth, then it interacts with the bottom reflectance in terms of a random absorption or reflectance (backwards) depending upon the outcome of another random number generation. Using the above general procedure, the Monte Carlo mathematical model allows the simulation of either direct or indirect irradiant light fields according to the 2-flow equations given by:

$$\frac{dE_d^w}{dz} = -(a+b)E_d^w(z) + bE_u^w(z) + cE_s^w(z) \qquad (1)$$

$$\frac{dE_u^w}{dz} = (a+b)E_u^w(z) - bE_d^w(z) - cE_s^w(z) \qquad (2)$$

$$\frac{dE_s^w}{dz} = -\alpha E_s^w(z) \qquad (3)$$

where a, b and α are the total absorption, backscatter and beam or collimated attenuation coefficients respectively. The conversion of the collimated irradiance, $E_s(\lambda)$ is proportional to the conversion rate, $c(\lambda)$ and this term may vary as a function of depth in the Monte Carlo (MC) model but is considered constant in the analytical model (Case II) we use it in the comparison of the MC results with the analytical model results in this paper. The above modified 2-flow equations can be derived from a general type of radiative transfer equation (RTE). By this we are generally referring to forms of model equations similar to that given below. For example, a version of a radiative transfer which describes the role of the absorption and scattering processes in a hydrosol is described by Priesendorfer[9] in equation (4) or:

$$\mu \frac{dL(z,\xi,\lambda)}{dz} = -c(z,\lambda)L(z,\xi,\lambda) + \int_{\Xi} L(z,\xi',\lambda)\beta(z,\xi' \to \xi;\lambda)d\Omega(\xi') + \beta(z,\xi' \to \xi,\lambda)L_c(z,\xi),$$

where $\mu=\cos\theta$ (cosine of the zenith angle), L is radiance ($Wm^{-2}sr^{-1}$), z depth (m) positive down, ξ is the travel direction of the light or photon stream along the vertical path z, at wavelength λ (nm), c is a beam attenuation (α) coefficient (absorption + scattering) (m^{-1}), Ξ indicates integration over all directions of a unit sphere, β is a volume scattering function[12,13,14] ($m^{-1}sr^{-1}$) which describes the amount of light originally heading in direction ξ' at depth z, elastically scattered into direction ξ (elastic scattering is used to denote scattering with no change of wavelength, whereas inelastic scattering is that scattering process which involves a change of wavelength or frequency). L_c is the collimated radiance ($Wm^{-2}sr^{-1}$), E_s is the collimated irradiance (Wm^{-2}), Ed (λ) and E_u (λ) are the upwelling and downwelling diffuse irradiance field terms (Wm^{-2}) in the water (w) or air (a). The first term on the right hand side of equation 4 above is the loss of radiant energy due to absorption or scattering (backwards or forwards) out of the path of the radiant energy flux. The 2nd and 3rd terms are gains due to the collimated or a path radiance being scattered within the path of the radiant energy (either diffuse or collimated). The irradiance models (1 through 3 above) have been analytically solved and results demonstrated by Bostater[1,2], and by using Monte Carlo techniques developed by Bostater[8,13,14]. Thus the RTE equation has been simplified into more readily solvable systems of differential equations, as witnessed in the well known[11], versions of the 2-flow equations given above. In their simplest case, these equations as given[1,2,3,8] above as a set of two or three coupled ordinary differential equations that describe the upwelling and downwelling irradiance in a unit volume of water of depth z. Similar equations and solutions for the non-homogeneous equations or the "layer approach" are presented by Bostater and Huddleston[15] and earlier by Bostater, McNally and Ma[16].

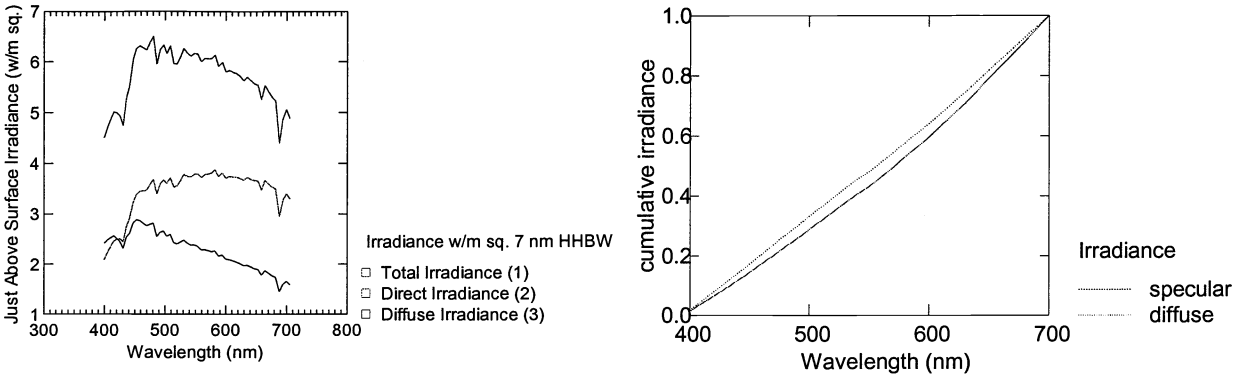

Figure1 (left) above shows the relative downwelling direct (specular) and indirect (diffuse) and total irradiance downwelling upon the water surface and Figure 2 (right) indicates the associated normalized cumulative irradiance curves upon the water surface. These irradiance (Wm^{-2}) and cumulative irradiance curves represent the energy from the sun, after atmospheric corrections are applied, and are used as inputs at the water surface to the analytical and Monte Carlo mathematical models described below.

2. METHODS

In comparing the analytical and Monte Carlo models, a portion of solar radiation that reaches the air-water interface is reflected using a diffuse or specular reflection coefficient. That fraction that is not reflected is then considered transmitted across the air water interface. The analytical model accounts for the wind-roughened effect upon the reflection. In the Monte Carlo model, the fraction of direct and indirect radiation is then refracted, giving it a new direction in the water.

This radiation attenuated as it proceeds down the water column. This attenuation is due to the absorbing and scattering properties of clear natural water according to the data from Smith & Baker[3]. Although both models allow for additional absorption and backscatter effects due to constituents in the water (total suspended sediments, phytoplankton, humic substances and lignin just to name a few), we will limit our discussion in this paper to comparing clear water property effects upon the synthetic water surface reflectance signatures. These attenuating parameters are analytically described by absorption and backscatter coefficients (a and b respectively). These coefficients are considered to be known and are considered to be quasi-inherent optical properties of the medium. Another inherent optical property used here is the beam attenuation coefficient (α) as described by Kirk[13]. Ultimately, these optical properties allow remote sensing to be used for the study of water quality constituents.

A uniform random number generation procedure is used to determine whether reflection or transmission occurs at the water surface interface for the Monte Carlo model. The direct light enters with a direction determined by the solar zenith angle and the diffuse light falls randomly onto the air-sea interface. The uniform random number used in the Monte Carlo model was derived from Bostater[8] and Wichmann & Hill[9], which uses Bostater's[8] embedded seed algorithmic procedure which makes calls to the time subroutine of the computer (SGI Octane dual processor FORTRAN 77) and substantially increases the time before the random number sequence is repeated. This random number generator subroutine was called in every part of the program, which required a random number. As such, this algorithm forms the basis of the numerical procedures that drives the photon flux in the Monte Carlo model.

Fresnel's equation is then used to determine the probability of reflectance off of the air/water interface. Fresnel's equation is defined as:

$$r = \frac{\sin^2(\theta_a - \theta_w)}{2\sin^2(\theta_a + \theta_w)} + \frac{\tan^2(\theta_a - \theta_w)}{2\tan^2(\theta_a + \theta_w)} \quad , \qquad (5)$$

where, θ_a and θ_w are the zenith angle of incidence of air and water respectively and r is the probability of the photon being reflected off of the water surface. A random number was then generated to determine if the photon penetrated the air/water interface. If the photon was successful in doing so, it's new angle of incidence was calculated based on Snell's law as follows:

$$\theta_w = \sin^{-1}\left(\frac{n_a}{n_w}\sin\theta_a\right) \quad , \qquad (6)$$

where n_a and n_w are the refractive indices of air and water, respectively. At this point, the photon has passed the air/water interface, and has a new direction vector. Figure 3 illustrates the above procedures for the photon to cross the air-sea interface or to be reflected.

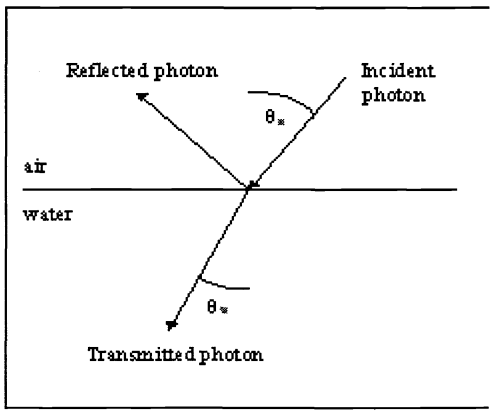

Figure 3. Illustration of photon air-sea interaction used in the Monte Carlo simulation for specular light.

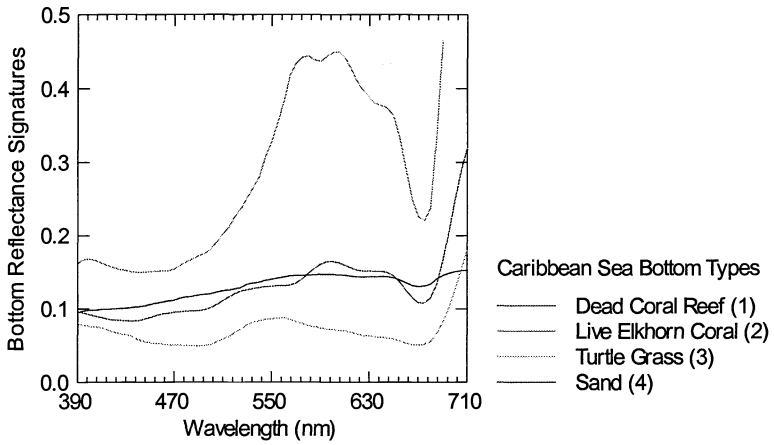

Figure 4. Bottom reflectance signatures collected from locations in the Caribbean Sea and used in the Monte Carlo & analytical model comparisons.

Once a photon or numerically tagged particle has entered the water column the photon optical pathlength P (m) must be defined. This quantity represents the maximum distance a photon will travel in the specified direction. Our goal in this paper is to develop a model that will assist with the calculation of the backscatter coefficient, b (1/m) and which is analogous to the backscatter coefficient used in equations 1 through 3 above. For example, one could use the form of equations 1 and 2 where we neglect (for brevity) the specular or direct component and divide equation 1 and 2 by $E_d(\lambda)$ and $E_u(\lambda)$ respectively, or given $dE_d(\lambda)/dz = -(a(\lambda)+b(\lambda))E_d(\lambda) + bE_u(\lambda)$, divide by $E_d(\lambda)$ to obtain attenuation $k_d(\lambda)$ for the downwelling field of irradiance. So $k_d(\lambda) = 1/E_d(\lambda)\ dE_d(\lambda)/dz = -(a(\lambda)+b(\lambda)) + b(\lambda)\ R(\lambda)$, or since , $b(\lambda)$ and $R(\lambda) < 1$ and $b(\lambda) < a(\lambda)$ (especially for clear natural waters) so $k(\lambda) = -(a(\lambda)+b(\lambda)) \cong a(\lambda)$. Now, using the relation $dE_d(\lambda)/dz = -kE_d(\lambda)$, and solving for $E_d(\lambda)$ and arranging one obtains the form for random number simulations used in this paper: $\ln[E_d(\lambda)/E_o(\lambda)] / -k(\lambda) = z \cong P$, where E_d/E_o is between 0 to 1 by definition, and valid where $b << a$ and $R < 1$ and $z \cong OP_d(\lambda)$ or the optical path length a photon travels before interaction at λ. The value 0 to 1 is obtained from the uniform random number generator after each appropriate interaction and is used in the Monte Carlo simulations discussed in this paper. An alternative method would be to include scattering as a function of the scattering coefficient (m^{-1}) to define P as:

$$P = \frac{1}{a + s(\xi)} \quad . \qquad (7)$$

Note that P is somewhat analogous to the inverse of Kirk's[13,16] beam attenuation coefficient c. The pathlength P does not represent the absolute distance traveled by the photon. It only indicates the maximum distance traveled by the photon before an interaction with a scattering or absorbing particle. The photon may, however, interact anywhere between its original position depth, h and the distance P with a hypothesized particle interaction. The depth of each particle is thus tracked until they are lost from the downwelling or upward flowing streams of photons.

In summary, a random number is generated which determines P and then another random number is generated to determine the "type" of the photon/particle interaction. This interaction can be either absorption or scattering. If the photon is absorbed, the photon is considered gone from the system, and a new photon is generated (for tracking from the air at λ_i, then the process

is repeated. If the photon is scattered, a random number is generated to determine either the angle of scattering (based upon a probability based scattering phase function) or is scattered forwards or backwards in the case of simulating the 2 flow equations. The random number generated is used in conjunction with a distribution function derived by fitting a specified probability based optical volume scattering distribution. The photon is given a new vector direction and the process of pathlength travel is repeated. This is continued until the photon is either absorbed by another particle, scattered again or the particle is tracked to the defined water column bottom depth. At the bottom, a random number is used to determine if the bottom absorbs the photon or reflected backwards using the known or measured bottom reflectance signature (0 to 1). If the random number is less than the specified $R_b(\lambda)$, the photon is lost due to bottom absorbtance or if greater than $R_b(\lambda)$, then the photon is available to begin its flow in the upwards direction, on terms of $E_u(\lambda)$. The same general procedure is used for photon/particle interaction to obtain the upward flowing light field (photon flux) at $E_u(\lambda)$.

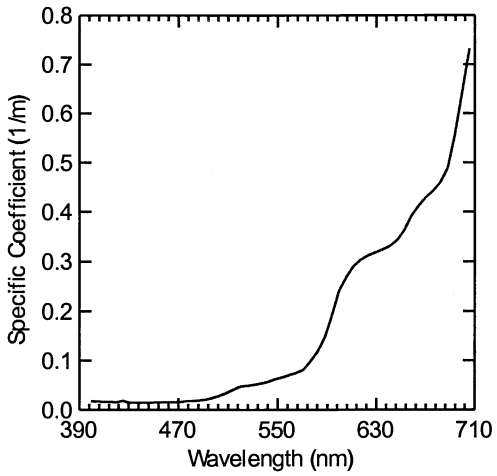

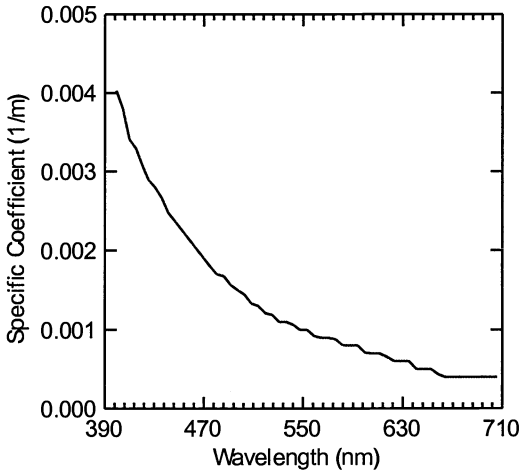

Figure 5 (left) and Figure 6 (right). The figure to the left indicates the values of the clear water absorption coefficients (after Smith & Baker, 1984) used in the Monte Carlo and the analytical model results. The backscatter signature (right) was calculated using a clear water reflectance spectrum for optically deep water and the data in figure 5.

Figure 3 shows the hyperspectral bottom reflectance signatures collected at stations in the Caribbean Sea for different bottom types. These signatures provide a comparison of the Monte Carlo and analytical models in the optically shallow water column simulations described below. Figure 5 shows the clear water values of the absorption coefficient as a function of wavelength after Smith & Baker[3]. This data was used in conjunction with a clear, optically deep, water surface reflectance to calculate a clear water backscatter coefficient. The resulting backscatter signature is shown in Figure 6 above. The data used to make these figures is also used as model inputs in the Monte Carlo and the analytical solutions to the 2 flow equations described by Bostater, Lamb and Ma[2].

The comparison of the Monte Carlo modeling approach with the analytical solution to the 2-flow equations will be based upon using the analytical solution technique described by Bostater, McNally and Ma[2]. The analytical mathematical model is based upon decoupling equations 1 and 2 and solving the resulting nonhomogeneous 2nd order differential equations with Cauchy type boundary conditions. This approach as outlined by Bostater, et al[1]. allows for the direct calculation of the reflectance at the air-sea interface using knowledge of the downwelling light $E_d(\lambda)$ at z=0 for the diffuse irradiance field, $E_s(\lambda)$ at z=0 for the collimated or direct sunlight irradiance from the sun (see Figure 2) the absorption and backscatter coefficients $a(\lambda)$ and $b(\lambda)$ and the bottom reflectance $R_b(\lambda)$. Results of the 2 modeling approaches are used to simulate the water surface reflectance signatures for clear optically deep water and optically shallow water influenced by Caribbean Sea bottom types (sand, Elkhorn coral, dead coral, submerged aquatic vegetation). The goal is to insure the hinge point can be simulated and that the clear water reflectance feature can be reproduced as well the influence of bottom type on the water surface reflectance signatures as demonstrated from actual measurements such as those shown in Figure 7 given below.

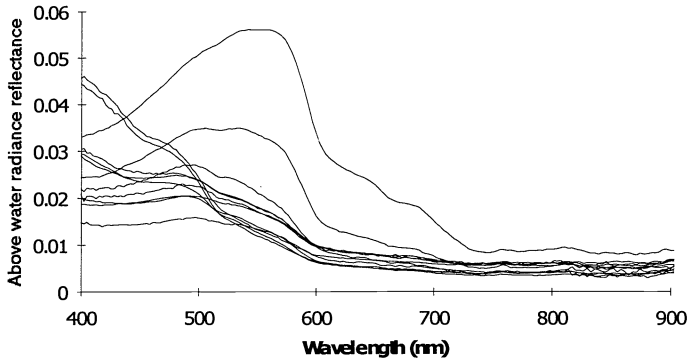

Figure 7. Characteristic water surface reflectance signatures collected at Cape Canaveral Florida coastal Atlantic Ocean surface water stations during March 1995 with a SE590 high resolution solid state spectrograph aboard the RV Delphinus. Note the characteristic exponentially decreasing clear water stations from the coastal stations with low 400-500 nm reflectance due to the presence of dissolved organic matter and the presence of the hinge point in the 500-530 nm characteristic of waters with suspended particulate matter. The goals of the Monte Carlo & analytical models are to scientifically explain and predict these hyperspectral signatures for use in water quality applications.

3. RESULTS

1

The results of the Monte Carlo and analytical models are shown below. Both models were run with pure water absorption and backscatter coefficients, bottom reflectance and downwelling direct and indirect irradiance as described above. Figure 8 shows the characteristic optically deep, clear water reflectance signatures.

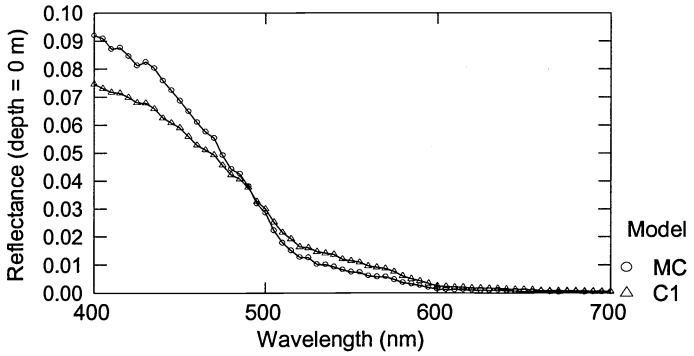

Figure 8. Simulated subsurface irradiance reflectance just below the air/water interface for optically deep water (1000 m depth). Monte Carlo (MC) versus 2 Flow Analytical Model pure water (C1). Backscatter & absorption coefficients used in the simulation of 10 million photons at 60 discrete wavelengths.

The results of the Monte Carlo and analytical models for clear optically deep water shows a striking similarity to measured water surface reflectance signatures as shown by Bostater, et al[1,2]. Both models were run with pure water absorption and backscatter coefficients, bottom reflectance and downwelling direct and indirect irradiance as described above.

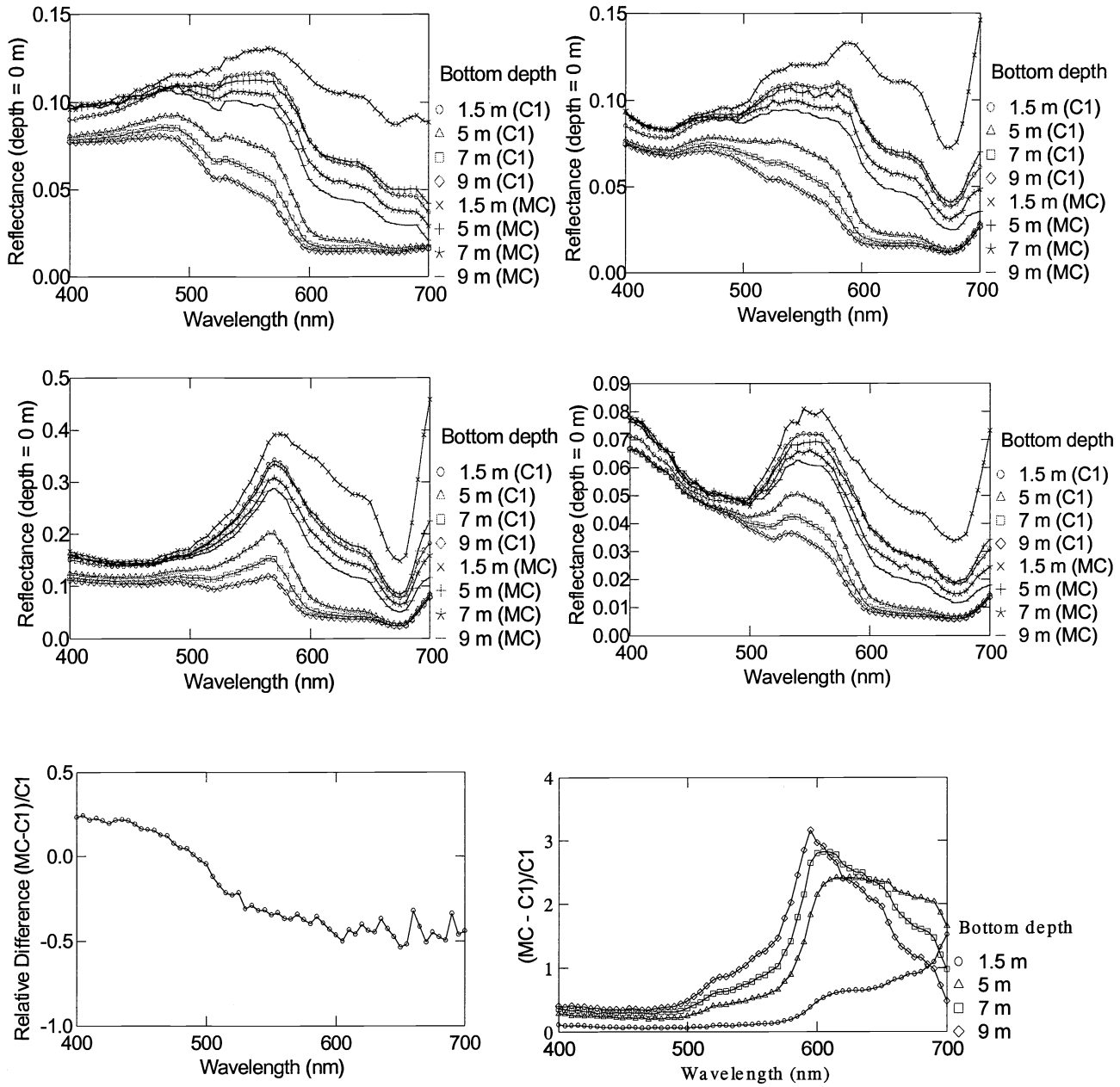

Figures 9-14. The top 4 graphs compare the Monte Carlo model with the analytical model for various water types. Figure 9 (top left) are the results with a Caribbean Sea sand bottom. Figure 10 (top right) shows model results for a dead coral bottom type. Figure 11 (middle left) indicates results for live Elkhorn coral bottom. Figure 12 (middle right) is the results for the sea grass (Turtle Grass) bottom. Figure 13 and Figure 14 indicates the relative difference between the two models for the clear water simulations and the Elkhorn coral model comparisons at various simulated water depths.

One use of a Monte Carlo model in remote sensing research is exploring how the reflectance and absorption coefficients are related to the backscatter coefficients. This is especially important since backscatter coefficients are difficult to measure directly, compared to reflectance and absorption. A simplified method for calculating backscatter coefficients has been given by Morel and Prieur[18] and others as:

$$R = C\, b/a, \qquad (8)$$

where C is a coefficient of proportionality that has been shown to be a function of solar zenith angle Kirk[13]. Kirk [13] has demonstrated by Monte Carlo methods that for waters with a b/a value between 1 and 5, and an incident sun zenith angle of 45, the proportionality constant C had a value of 0.083. This was derived by relating radiance reflectance (L_u/E_d) to b/a. The Monte Carlo (MC) model approach described in this paper and the Case II[6] analytical model (C1) are based upon irradiance reflectance output (E_u/E_d) and in these models we assume a uniform radiance distribution of upwelling light. One can relate radiance reflectance and irradiance reflectance as shown below to b/a by a separate factor (sometimes-called Q) or L_uQ/E_d or incorporating Q into C above:

$$E_u/E_d = L_u/E_d = C'\, b/a \qquad (9)$$

Kirk's coefficient of proportionality as shown above (C') is then approximately equal to 0.26 for irradiance reflectance. Other research has suggested a value closer to 0.33 and Bostater et al[6] have suggested a value closer to 0.29 based upon the analytical model and data collected off Central Florida. Both the C1 and MC models have average values of 0.04 and 0.07 respectively (Figure 15) for b/a values ranging between 1 and 5.

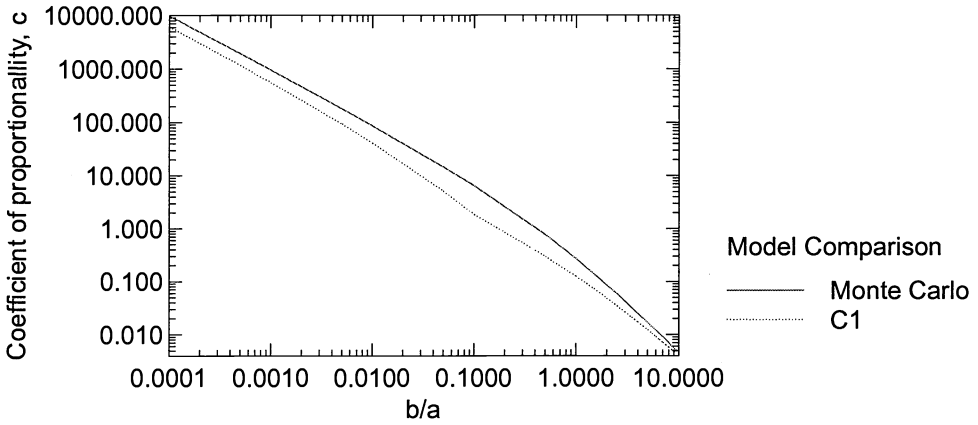

Figure 15. Comparison between the calculated coefficient of proportionality between simulated reflectance (R) and the ratio b/a for the Monte Carlo and the analytical model (C1) outputs.

The simulations comparing the Monte Carlo model and analytical model with various water depth and bottom reflectance types were made with the described pure water values of total absorption and backscatter coefficients (figures 9-12). Another test of the model is to attempt to reproduce a hinge point as suggested in figure 7. This type of feature exists in the measured reflectance spectra one encounters when measuring different waters with various water concentrations of constituents such as chlorophyll-a, dissolved organic matter and suspended particulates. Figure 16 is presented in order to demonstrate the ability of the hyperspectral Monte Carlo model to simulate the hinge point in optically shallow water influences by bottom reflectance $R_b(\lambda)$.

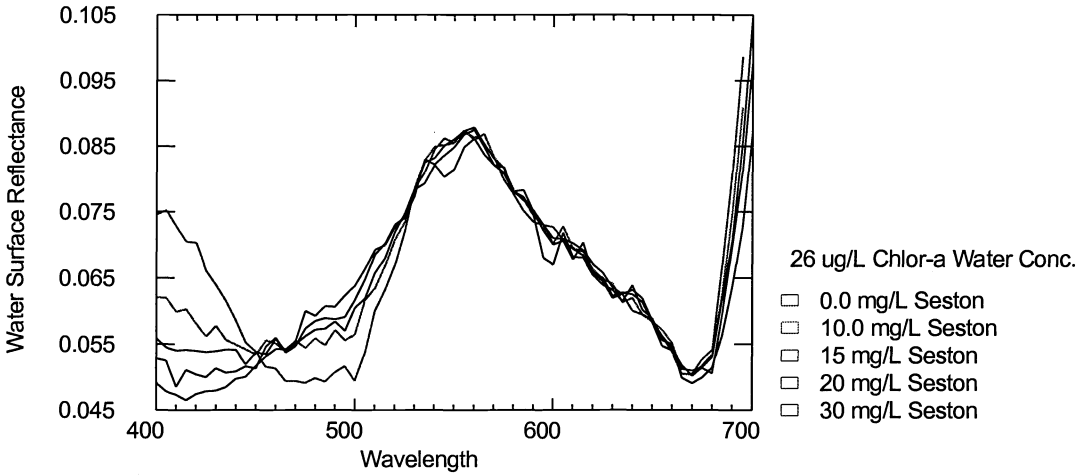

Figure 16. Hyperspectral synthetic Monte Carlo modeled reflectance signatures. Note the occurrence of a "hinge point" with the high chlorophyll-a concentration and the effect of varying seston concentrations. The decrease at approximately 660 to 685 nm is due to the chlorophyll-a concentration absorption effect in conjunction with the effect of the live Elkhorn coral bottom type in optically shallow water.

4. DISCUSSION

The above mathematical models were compared with the goal to provide a framework for developing refined techniques to calculate the backscatter coefficient for use in simplified remote sensing models based upon radiative transfer theory. As shown in the figures of the relative difference between the two models (Monte Carlo and the analytical solution) further refinements in the Monte Carlo model are needed to reduce relative errors as a function of wavelength. However the general trend in being able to generate hyperspectral synthetic signatures with a "hinge point" characteristic is a positive model development, as well as being able to include the influence of optically shallow bottom types. Future work and refinements in the model procedures will include inclusion of probabilistic based scattering phase functions, influence of the beam attenuation[19] and associated conversion coefficient, temperature effects[21] and sensitivity of non lambertian bottom types in CASE II and CASE III water types[20].

5. ACKNOWLEGEMENTS

NASA, Kennedy Space Center, Florida Tech and Dynamac Corp. assisted in financial support to the Florida Tech graduate student M. Gimond. Support for undergraduate student activities of M. Campbell was provided by the National Science Foundation. Computers, aircraft & ground based remote sensing equipment as well as software central to this research has been provided by KB Science and S&C Services.

6. REFERENCES

1. Bostater, C., Ma, W., Lamb, A., "Simulating radiative transfer in aquatic systems and contrasting results from ambient environmental spectroscopy: estuarine & near coastal waters, In: Proceedings, Int. Symposium On Spectral Sensing Research, USACE, Vol. 2, pp. 673-682, 1994.
2. Bostater, C., Ma, W., McNally, T., Gimond M., Lamb, A., "Application of an optical remote sensing model," SPIE, Vol. 2586, pp. 32-43, 1995.
3. Smith, R., Baker, K., "Optical properties of the clearest natural waters", Applied Optics, Vol. 20, pp. 177-184, 1981.
4. Bostater, C., Gimond, M., "Methodology evaluation for remotely estimating water quality parameters in estuarine waters," SPIE, Vol. 2586, pp. 14-25, 1995.

5. Bostater, C., "Specific absorption and backscatter coefficient signatures in southeastern Atlantic coastal waters", SPIE, Vol. 3496, pp. 196-200, 1998.
6. Ma, W., "An analytical two-flow model to simulate the distribution of irradiance in coastal waters with a wind – roughened surface and bottom reflectance", Ph.D. Dissertation, Florida Tech, pp. 299, 1997.
7. Greg, W., Carder, K., "A simple spectral solar irradiance model for cloudless marine atmospheres", Limnology & Oceanography, Vol. 35(8), pp. 657-675, 1990.
8. Bostater, C., On simulating the active vertical motion of Morone Saxatilis in the estuarine environment", Ph.D. Diss., University of Delaware, pp. 207, 1989.
9. Wichmann, J., Hall, C., "A random number generator routine in Pascal", Byte, 1987.
10. Priesendorfer, R., *Hydrologic Optics*, Vol. I-VI, NOAA/ERL, Honolulu, HI, pp.1757, 1978.
11. Kubelka, P., Munk, F. "Ein Beitrag zur optik der Farbanstriche," *Z. Tech. Physik* 12, pp. 593, 1931.
12. Petzold, T., "Volume scattering functions for selected ocean waters," SIO Ref. 72-78, In: *Light in the Sea*, Edited by J.E. Tyler, Dowden, Hutchinson & Ross, Stroudsberg, pp. 150-174, 1977.
13. Kirk, J., *Light and Photosynthesis in Aquatic Ecosystems*, 2nd Edition. Cambridge University Press 1994.
14. Haltrin, V.L., "Monte Carlo Modeling of Light Field Parameters in Ocean with Petzold Laws of Scattering," 4th Int. Conference on Remote Sensing for Marine & Coastal Environments, Orlando, Florida, pp. 502-508, 1997.
15. Bostater, C., Huddleston, L., "Layered analytical radiative transfer model for simulating water color of coastal waters and algorithm development", SPIE, (this volume), pp. 9, 2000.
16. Bostater, C., McNally, T., Ma, W., "Modeling of the underwater light field and its effect on temperature, stability and momentum," SPIE, Vol. 2959, pp. 171-179, 1996.
17. Kirk, J.T.O., "Monte Carlo Study of the Nature of the Underwater Light Field in, and the relationship between Optical Properties of, Turbid Yellow Waters," Australian Jrnl. Marine & Freshwater Research. 32, pp. 517-532, 1981.
18. Morel, A., Prieur, L., "Analysis of variations in ocean colour," Limnology and Oceanography," 22, pp. 709-22, 1977.
19. Avrillier S., Tinet, E., Delettre E. "Monte Carlo simulation of collimated beam transmission through turbid media," Journal de Physique 51, pp. 2521-2542, 1990.
20. Jerlov, N., *Marine Optics*, Elsevier Oceanography Series, Vol. 14, 1976, 231 pp., 1976.
21. Pegau, W., Zanevald, J., "Temperature-dependent absorption of water in the red and near-infrared portions of the spectrum," Limnol. Oceanogr. 38(1), pp.188-19, 1993.